Published online August 24, 2006

Quantifying the Pore Size Spectrum of Macropore-Type Preferential Pathways under Transient Flow

K.-J. S. Kung,* E. J. Kladivko, C. S. Helling, T. J. Gish, T. S. Steenhuis, and D. B. Jaynes

ABSTRACT

It is well known that there is a spectrum of pores in a soil profile. The conventional use of a single lumped value of soil hydraulic conductivity to describe a spectrum of hydraulically active pores may have unintentionally impeded the development of field-scale chemical transport theory and perhaps indirectly hindered the development of management protocols for chemical application and waste disposal. In this study, three sets of four field-scale tracer mass flux breakthrough patterns measured under transient unsaturated flow conditions were used to evaluate the validity of an indirect method to quantify equivalent pore spectra of macropore-type preferential flow pathways. Results indicated that there were distinct trends in how pore spectra of macropore-type preferential flow pathways changed when a soil profile became wetter during a precipitation event. This suggests that the indirect method has predictive value and is perhaps a better alternative to the lumped soil hydraulic conductivity approach in accurately determining the impact of macropore-type preferential flow pathways on water movement and solute transport under transient unsaturated flow conditions.

The distribution of soil pore sizes is one of the most basic of all soil physical properties. It is well known that soil pores have a spectrum of equivalent radii. Soil pore spectrum affects infiltration, drainage, soil aeration, surface runoff, soil erosion, and chemical leaching. Arguably, it even influences the ability to determine the impact of various chemical management strategies on surface and subsurface water quality. In soil science, the soil hydraulic conductivity has been traditionally used as a basic soil physical property to describe the impact of soil pores on water movement and solute transport. Darcy (1856) first introduced this parameter when he demonstrated that the water flux through a saturated sand column was proportional to a potential gradient. Buckingham (1907) later extended the experiments and introduced unsaturated soil hydraulic conductivity.

Frequently ignored is the fact that soil pores in natural heterogeneous soils are anisotropic. As a result, the soil hydraulic conductivity is a second-rank tensor with nine different hydraulic conductivity vectors (Bear, 1972). This complexity might not influence the overall water movement, but it could have a significant impact on the pore connectivity and hence the mixing of contaminant transport. Since no methods exist for reliably quantifying all of these nine vectors, a single lumped parameter is typically used to describe the soil hydraulic conductivity as a function of soil matric potential or water content. In essence, the method lumps the contributions of all pores across a plane on water movement, yielding a single hydraulic conductivity value for a specific condition (e.g., 1 m h^{-1} for coarse sand or well-aggregated soils vs. 1 cm d^{-1} for nonstructured clayey soils).

Another issue is how large the elementary representative volume should be from which the lumped parameters are determined. If the lumped parameters are determined at a scale that does not represent field-scale flow conditions, the results may have limited application (Khan and Jury, 1990; Jensen and Refsgaard, 1991). Thus, the lumped hydraulic conductivity is a simplified approximation of a complex flow scenario measured at a specific scale that could have additional problems when extended to larger scales of observations. This partly explained why unrealistically large dispersion coefficients were often necessary to obtain a good fit with the chemical transport solutions when field-scale heterogeneities could not be captured by a lumped hydraulic conductivity (Gelhar, 1987).

Using a single lumped value of soil hydraulic conductivity to describe the contribution of a spectrum of hydraulically active pores has led to considerable debate over which of the solute transport approaches should be used (van Genuchten and Parker, 1984; Barry and Sposito, 1989; Jardine et al., 1989; Novakowski, 1992). When a soil profile is relatively dry, the matric potential would restrict water movement in the smaller matrix pores. These matrix pores among soil primary particles are self-similar and interconnected. Transport through these matrix pores tends to cause a thorough solute mixing. Hence, there is a well-defined chemical front with a characteristic velocity and spreading. Under this scenario, a lumped soil hydraulic conductivity and dispersivity can very successfully describe the solute transport process (Cassel et al., 1975; Wierenga et al., 1991). However, there are situations (e.g., a relatively wet soil profile or a high intensity precipitation) when water and contaminants can move through macropore-type preferential pathways. Under this scenario, because chemicals in macropores generally would not mix thoroughly with those in the matrix pores, a lumped soil hydraulic conductivity and dispersivity cannot describe the solute transport process (Jaynes et al., 2001).

Compensating for transport through macropores eventually evolved into the development of "two-region"

K.-J.S. Kung, Dep. Soil Science, Univ. of Wisconsin, Madison, WI 53706-1299; E.J. Kladivko, Dep. Agronomy, Purdue Univ., West Lafayette, IN 47907; C.S. Helling, Sustainable Perennial Crops Lab., and T.J. Gish, Hydrology and Remote Sensing Lab., USDA-ARS, BARC-W, Beltsville, MD 20705-2350; T.S. Steenhuis, Dep. Biological and Environmental Engineering, Cornell University, Ithaca, NY 14850; D.B. Jaynes, National Soil Tilth Lab., USDA-ARS, Ames, IA 50011. Received 10 Jan. 2006. *Corresponding author (kskung@wisc.edu).

Published in Vadose Zone Journal 5:978–989 (2006).
Special Section: Parameter Identification and Uncertainty Assessment in the Unsaturated Zone
doi:10.2136/vzj2006.0003

Abbreviations: PFBA, pentafluorobenzoic acid; *o*-TFMBA, *o*-trifluoromethyl benzoic acid; 2,6-DFBA, 2,6-difluorobenzoic acid.

models (Barenblatt et al., 1960; van Genuchten and Wierenga, 1976; Gish and Jury, 1983; van Genuchten et al., 1984; Gerke and van Genuchten, 1993) and "multiple domain" models (Hutson and Wagenet, 1995; Gwo et al., 1995). These approaches allow chemicals to enter and be transported through different domains to alleviate the drawback of lumped soil hydraulic conductivity and dispersivity. However, it has remained unclear how to define the boundary and interaction among domains. Furthermore, a major hurdle has been measuring the physical parameters within each domain independently. On the other hand, the transfer function approach was proposed to simulate chemical transport through heterogeneous soils (Jury, 1982). This latter approach suggests that, because how the complex pore connectivity would influence the field-scale solute transport is holistically reflected on the solute breakthrough curve, it is not necessary to independently measure key descriptive parameters such as soil hydraulic conductivity, pore interconnectivity, and chemical dispersivity. As long as the representative field-scale solute breakthrough curves can be measured, a probability density function can be derived to successfully predict field-scale contaminant transport (Jury et al., 1986; Beven and Young, 1988; Scotter and Ross, 1994).

One of the most fundamental breakthroughs in modern physics was the discovery of how to separate, manage, and take advantage of a spectrum of electromagnetic waves in different wavelengths. Similarly, in soil and environmental sciences, there is an urgent need to develop methodology to quantify the soil pore spectrum. The smaller soil pores serve as storage, and larger pores are conduits for transport pathways. The protection of water quality is often dictated by how to prevent the entry of chemicals into the pathways with large pore radii. Without a solid grasp of this critical information, it will be difficult to develop sound management practices for proper pesticide usage or effective waste disposal. Durner and Flühler (1996) conducted numerical experiments and concluded that a continuous pore spectrum must be considered to simulate accurately chemical transport associated with macropores. Results from field-scale tracer mass flux breakthrough experiments conducted by Kung et al. (2000a, 2000b), Jaynes et al. (2001), Gish et al. (2004), and Kung et al. (2005) revealed that not only did macropore-type preferential flow paths dictate deep chemical leaching, but also more macropore-type preferential flow paths became hydraulically active as a soil profile became wetter. Kung et al. (2005) contended that to predict the impact of these macropore-type preferential flow paths on solute transport, it is critical to first quantify the pore spectrum of these pathways.

Currently, there is no reliable way to directly and accurately quantify the field-scale pore spectrum of macropore-type preferential flow paths in a soil profile. Kim et al. (2005) proposed a method to predict the chemical flux through macropore-type preferential pathways. However, because it was assumed that the transport mechanism was governed by the convection–dispersion equation, their approach could only estimate lumped parameters such as soil hydraulic conductivity and dispersion coefficient. Kung et al. (2005) proposed an indirect methodology by using field-scale tracer mass flux breakthrough patterns to quantify equivalent pore size spectrum of flow pathways. Their two central premises were that: (i) the impacts of key descriptive parameters such as soil hydraulic conductivity, pore connectivity, and chemical dispersivity on solute transport were holistically reflected in the chemical mass flux breakthrough patterns; and (ii) mass flux breakthrough through macropore-type preferential flow paths can be conceptualized as convective transport through capillary tubes.

The first premise was based on the holistic conceptualization embedded in the transfer function model. The second premise was based on an observation from field-scale tracer mass flux experiments (Gish et al., 2004; Kung et al., 2005), where the tails of chemical mass flux breakthrough patterns of conservative tracers through macropore-type preferential flow paths have slopes of -3 on log-log scale. The tail of a convective transport pattern of a conservative tracer through a capillary tube also has a slope of -3 on log-log scale. The tracer mass flux experiments by Gish et al. (2004) and Kung et al. (2005) were conducted under steady-state infiltration conditions. Under transient flow conditions, it was not clear if the indirect methodology proposed by Kung et al. (2005) was still valid. The objective of this study was to quantify the field-scale pore size spectrum of macropore-type preferential pathways under transient flow conditions.

MATERIALS AND METHODS

Three sets of tracer mass flux breakthrough patterns were used as input in our analysis. The first set was from a field experiment conducted at the South East Purdue Agricultural Center in Butlerville, IN by Kung et al. (2000a). The soil is Clermont silt loam soil (fine silty, mixed mesic Typic Ochraqualf). This loess soil is typical of the southern portion of Midwest Corn Belt soils, extending from southwestern Ohio, across southern Indiana and southern Illinois, through Missouri, into southern Iowa and eastern Kansas (Kladivko et al., 1999). In that study, four conservative tracers (bromide, pentafluorobenzoic acid [PFBA], *o*-trifluoromethyl benzoic acid [*o*-TFMBA], and 2,6-difluorobenzoic acid [2,6-DFBA]) were sequentially applied during a 10-h irrigation with 3 mm h^{-1} intensity. These benzoic acids were the same as those tested by Bowman and Gibbens (1992) and had identical transport property as that of bromide (Kung et al., 2000a). Bromide was sprayed on a narrow 1.5 by 24 m strip offset 0.3 m from a tile line shortly before irrigation started, while PFBA, *o*-TFMBA, and 2,6-DFBA were sequentially applied at 2, 4, and 6 h thereafter to the same area, respectively. The tile flow was continuously measured, and water samples were collected to determine mass flux breakthrough patterns of the four tracers. This experimental scheme was to explore how water and tracers would move through the larger end of the pore spectrum of macropore-type preferential flow paths as a soil profile became wetter. The measured tracer mass flux breakthrough patterns (normalized by the total mass applied) are shown in Fig. 1.

Five days after the main tracer leaching experiment from the first irrigation described above, we assumed that most of the four tracers that had not leached out had entered soil matrix pores. We then applied a second irrigation of 3 mm h^{-1} intensity and 10-h duration to the same field. This was to determine if subsequent precipitation events would cause similar deep leaching of chemicals already entered into soil matrix

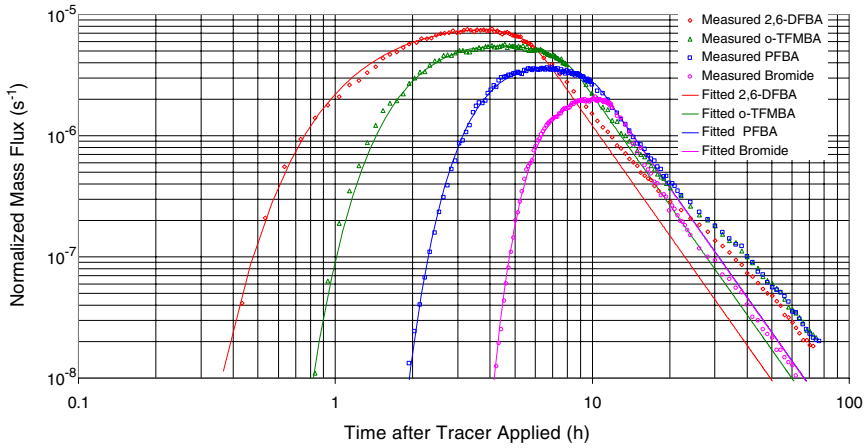

Fig. 1. Normalized tracer mass flux breakthrough patterns. The open symbols were measured values from Kung et al. (2000a). The solid lines are the best-fitted breakthrough curves based on pore spectra with parameters shown in Table 3.

pores. The tile flow was continuously measured and water samples were collected to determine mass flux breakthrough patterns of the four tracers applied earlier. The irrigation scheme as well as the equipment and methodology to measure tile flow and collect water samples were identical to those described in Kung et al. (2000a). Four days after the second irrigation event, a third and final irrigation of 3 mm h^{-1} intensity and 10-h duration was applied to the same field. Again, the tile flow was continuously measured and water samples were collected to determine mass flux breakthrough patterns of the four tracers. There was no natural precipitation during the second and the third leaching events.

The purpose of these last two irrigation events was to collect tracer mass flux breakthrough patterns to quantify the pore spectra of macropore-type preferential flow pathways that would contribute to the deep leaching of tracers already entered into matrix pores of a soil profile. We chose to use a tile drain monitoring facility to achieve high mass recovery (Gish et al., 2004; Kung et al., 2005) as well as to avoid spatial variability associated with other sampling protocols (Ju et al., 1997; Williams et al., 2003). The mass flux for each tracer at a specific time was calculated by multiplying the measured tile flow rate and tracer concentration. Then, the mass flux of each tracer was normalized by the total applied mass of that tracer from the first irrigation event by Kung et al. (2000a). The major findings from these experiments are discussed. Then, a methodology proposed by Kung et al. (2005) is used to analyze these three sets of tracer mass flux breakthrough patterns to quantify the field-scale pore size spectrum of macropore-type preferential pathways under transient condition.

RESULTS

The measured tracer mass flux breakthrough patterns from the second and the third irrigation events are shown in Fig. 2 and 3, respectively. In Fig. 1, there are significant differences in tracer arrival times for the four tracers from the first irrigation event. In contrast, the differences in breakthrough among the four tracers in Fig. 2 and 3 are very small. As a matter of fact, the measured mass flux breakthrough patterns of PFBA, *o*-TFMBA, and 2,6-DFBA from the second and the third irrigation event had almost identical shapes, while that of bromide was consistently slightly lower.

The mass leached during each irrigation, (i.e., the area under each breakthrough curve in Fig. 1–3) are listed in Table 1. The fact that much less mass is leached out in the subsequent irrigation events suggested that after tracers entered into the fine pores of a silty soil profile, they become less susceptible to deep leaching through macropore-type preferential flow paths. Because bromide was applied to a dry soil surface and entered into the smallest pores, it consistently had the least deep leach-

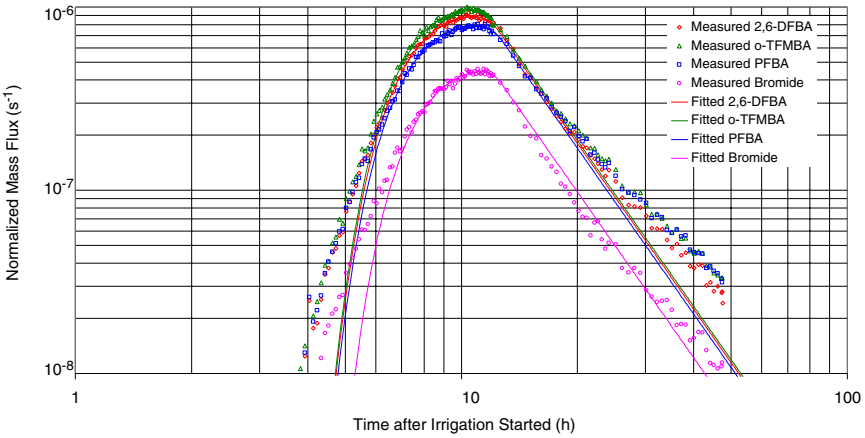

Fig. 2. Normalized tracer mass flux breakthrough patterns. The open symbols were measured from the second irrigation event. The solid lines are the best-fitted breakthrough curves based on pore spectra with parameters shown in Table 4.

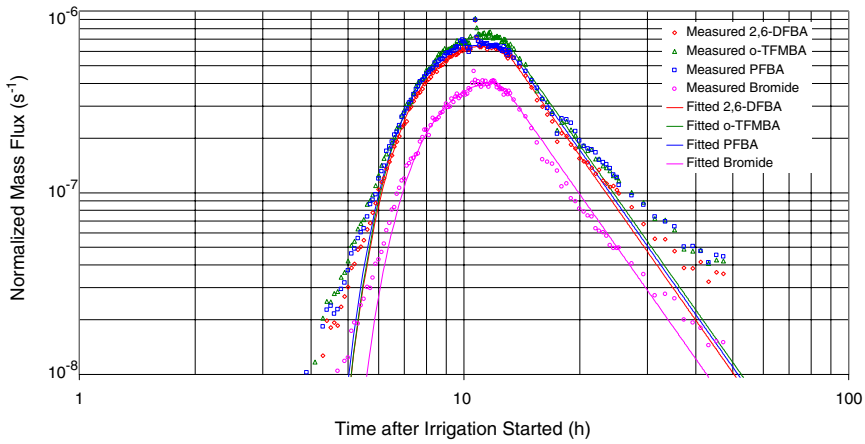

Fig. 3. Normalized tracer mass flux breakthrough patterns. The open symbols were measured from the third irrigation event. The solid lines are the best-fitted breakthrough curves based on pore spectra with parameters shown in Table 5.

ing in each irrigation event. Similar results were found by Shipitalo et al. (1990), Jaynes et al. (1992), Edwards et al. (1993), and Kladivko et al. (1999).

DATA ANALYSIS

In this section, we use the three sets of mass flux breakthrough patterns of bromide, PFBA, *o*-TFMBA, and 2,6-DFBA (Fig. 1–3) to quantify the equivalent pore spectrum of macropore-type preferential pathways contributing to the tracer transport under transient flow conditions. Kung et al. (2000a) already argued that the first set of mass flux breakthroughs were caused by chemical transport through macropore-type preferential pathways. Jaynes et al. (2001) demonstrated numerically that tracer leached out from a similar soil profile by an irrigation event of 3 mm h^{-1} intensity and 10-h duration was not transported through soil matrix pores. Therefore, mass flux results shown in Fig. 2 and 3 suggest that all four tracers leached out during the second and the third irrigations were also transported through preferential flow paths, although most of the tracers had entered into matrix pores of the soil profile.

To apply the indirect methodology proposed by Kung et al. (2005) to quantify the equivalent pore spectrum under transient flow conditions it was necessary to first examine whether the tail of mass flux breakthrough patterns shown in Fig. 1–3 also had a slope of −3 on a log-log scale. Among the 12 individual tracer mass flux breakthrough patterns collected from the three irrigation events, only those of *o*-TFMBA and 2,6-DFBA from the first irrigation did not have some parts of their tails with slopes nearly equal to −3. The remaining 10 mass flux breakthrough patterns with tail slopes nearly equal to −3 are plotted in Fig. 4. Each tail slope and its R^2 value of power fit are shown beside each tracer's label. Generally speaking, bromide breakthrough had the longest period with its tail slope equal to −3. For example, the entire bromide tail from the first irrigation had a slope of −3.01 and more than one-half of the bromide tails from the second and the third irrigation events had slopes of −3.02.

Table 1. Total mass leached out divided by the total mass applied.

Irrigation event	Bromide	PFBA	*o*-TFMBA	2,6-DFBA
	%			
1	7.04	13.9	18.7	19.7
2	1.60	3.30	3.78	3.43
3	1.59	3.32	3.43	2.98

Tail slopes of mass fluxes in Fig. 4 range from −2.94 to −3.05, with R^2 values between 0.972 and 0.998. This suggested that tracers transported through macropore-type preferential flow paths under transient conditions can be also conceptualized as transported through cylindrical tubes. Thus it is valid to use the indirect methodology proposed by Kung et al. (2005) to quantify the equivalent pore spectrum of macropore-type preferential pathways contributing to the tracer transport under transient conditions. Why bromide had a longer period with its tail slope nearly equal to −3 and why *o*-TFMBA and 2,6-DFBA from the first irrigation did not have tails with slopes equal to −3 will be discussed later.

We used governing Eq. [1], [2], and [3], derived by Kung et al. (2005), to describe convective mass flux, M, through capillary tubes.

$$M(r,t) = 0 \text{ for } 0 \le t \le \frac{4\upsilon L}{gr^2} \qquad [1]$$

$$M(r,t) = \pi r^2 \frac{r^2 g}{8\upsilon} C \left[1 - \left(\frac{4\upsilon L}{gtr^2}\right)^2\right] \text{ for } \frac{4\upsilon L}{gr^2} + t_p \ge t \ge \frac{4\upsilon L}{gr^2} \qquad [2]$$

$$M(r,t) = \frac{2\pi\upsilon L^2}{g}\left[\left(\frac{1}{t - t_p}\right)^2 - \left(\frac{1}{t}\right)^2\right] \text{ for } t \ge \frac{4\upsilon L}{gr^2} + t_p \qquad [3]$$

where r is pore radius of a capillary tube (m), t is time (s), υ is kinematic viscosity ($m^2\ s^{-1}$), L is length of a capillary tube (m), g is gravitational constant ($m\ s^{-2}$), C is input chemical concentration of a chemical pulse ($mg\ m^{-3}$), and t_p is duration of application of the short chemical pulse(s). These three equations indicate that

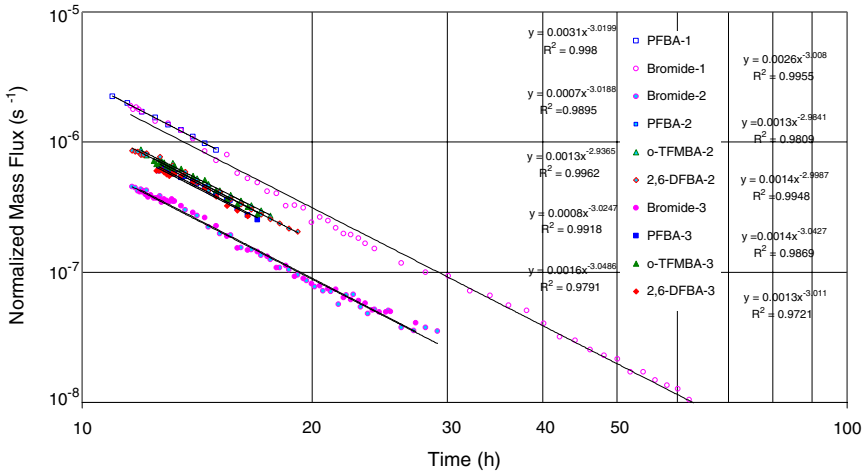

Fig. 4. The portions of normalized tracer mass flux breakthrough patterns that had tail slopes nearly equal to −3 on log-log scale. The suffix of each label indicates irrigation event (e.g., PFBA-1 indicates the tracer breakthrough curve from the first irrigation event).

mass flux through a capillary tube is composed of three stages. First, there is no breakthrough when time is less than the chemical arrival time, $4\upsilon L/(g\ r^2)$. Then, the second equation dictates the initial breakthrough of the pulse. Finally, the third equation describes the stage after solute-free water starts to replace the chemical pulse.

To describe a pore spectrum of equivalent capillary tubes, Kung et al. (2005) proposed an expression with six parameters. We slightly modified their expression as follows:

$$F(r) = A\left(\frac{r_2}{r}\right)^{\alpha} e^{-(r_1/r)^{\gamma}} e^{-(r/r_2)^{\eta}} \qquad [4]$$

We introduced two characteristic pore sizes, r_1 and r_2, which determine the lower and upper boundaries of the pore spectrum, respectively. The other terms were as defined by Kung et al. (2005); that is, A is the overall magnitude of pore frequency, α dictates the overall slope of pore frequency distribution between r_1 and r_2, γ and η dictate how fast the pore frequency drops to zero near r_1 and r_2, respectively. How these six parameters influence the shape of a pore spectrum is demonstrated in Fig. 5. Values of the six parameters of each spectrum are listed in Table 2.

We conceptualized that a soil profile has many capillary pores. For a combination of six values, a spectrum can be constructed to represent the frequency distribution of these pores. Then, for each capillary pore with radius r, one could use the three mass flux equations to calculate a breakthrough pattern. By summing all breakthrough patterns from all capillary pores, one could construct an overall mass flux breakthrough pattern for the entire soil profile. However, if the combination of six parameters were not correct, the calculated and measured breakthrough patterns would not match. Based on best curve fitting with least squares, one could systematically and sequentially adjust each of the six parameters so that a calculated breakthrough pattern will eventually match the measured breakthrough pattern. This procedure produced parameters for each of the 12 tracer mass flux breakthrough curves shown in Fig. 1–3.

The key question is whether there is any distinct trend among these parameters within each infiltration event. Without definite trends in how these six parameters changed during an infiltration event, the indirect method of Kung et al. (2005) would lack predictive power and hence be of marginal value. When Kung et al. (2005) proposed the indirect approach to quantify pore spectrum of

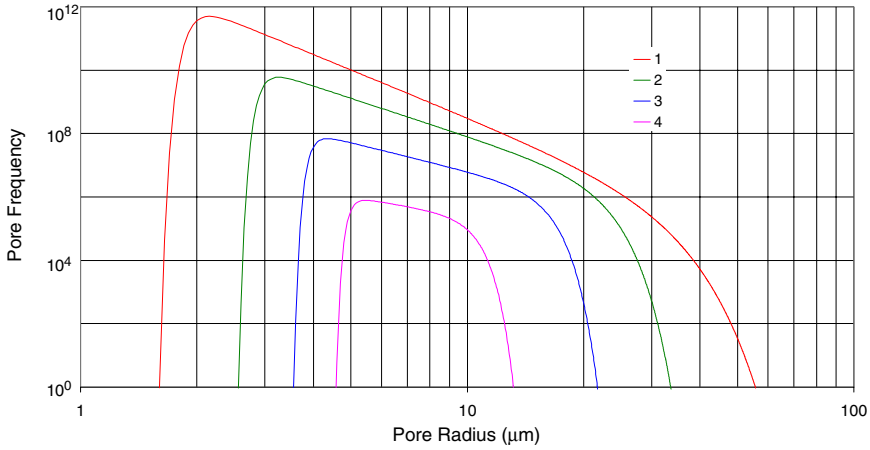

Fig. 5. Four hypothetical pore spectra to demonstrate how each parameter would alter the shape of a spectrum.

Table 2. Parameters of four hypothetical pore spectra.

Spectrum	α	η	γ	r_1	r_2	A
1	5	3	15	2	25	1.E+12
2	4	5	20	3	20	1.E+10
3	3	7	25	4	15	1.E+08
4	2	9	30	5	10	1.E+06

macropore-type preferential flow pathways, their breakthrough curves were measured under three steady-state infiltration conditions. Three data points for each parameter were not sufficient to demonstrate explicitly whether there were distinct trends. The fitted breakthrough curves are shown as solid lines in Fig. 1 through 3, while the parameters of each pore spectrum are shown in Tables 3, through 5.

The shapes of the equivalent pore spectra based on parameters listed on Table 3 are shown in Fig. 6. To determine the trend, the relationships among the parameters of four spectra from the first irrigation event shown in Fig. 6 and Table 3 are analyzed. It was during this event when the four conservative tracers were sequentially applied (i.e., bromide was sprayed shortly before irrigation started, while PFBA, *o*-TFMBA, and 2,6-DFBA were applied at 2, 4, and 6 h thereafter). The four mass flux breakthrough curves from this event shown in Fig. 1 demonstrate faster arrival time and higher recovery of the four sequentially applied tracers. This indicated that increasingly more macropore-type preferential pathways with larger equivalent pore radii became hydraulically active as the soil profile became wetter. The relationships among the six parameters from this event could reflect whether there are distinct trends.

As shown in Fig. 7A, α is linearly related to the time when a tracer is applied after the initiation of irrigation. The four conservative tracers were sequentially applied when the soil profile near the surface became wetter and wetter. Therefore, one can say that α is dictated by the soil water content of the soil profile when a chemical is applied. Figures 7B, 7C, and 7D show that the other five parameters are all related to α. How increasingly more macropore-type preferential flow pathways—with larger and larger equivalent pore radii—become hydraulically active is all related to the soil water content near the surface. In other words, the fitted parameters were not some random values. Moreover, because all the other five parameters are related to α, the expression of the pore spectrum needs only one parameter (i.e., the Eq. [4] was overparameterized).

DISCUSSION

The very high R^2 values in Fig. 7A through 7D strongly suggest that Kung's indirect method is scalable in time domain and as such has predictive value. For example, based on the relationships shown in these four figures, one can predict the pore spectra that dictate mass flux breakthrough patterns if a tracer was applied at 1, or 3, or 5 h after irrigation started. Although the trends shown in Fig. 7A through 7D strongly suggest that the six parameters are all related, the regression equations shown in these figures are not absolute. For example, the regression equations in Fig. 7B are based on an exponential fit. However, one can also use a power or a polynomial fit to describe these relationships. This was because four or five data points were still not enough to accurately determine an exact relationship. Moreover, the value of α would eventually reach a plateau (instead of increasing indefinitely) as a soil profile eventually reached a steady-state condition. Furthermore, these regression equations were only to describe how macropore-type preferential pathways became hydraulically active under 3 mm h^{-1} rain intensity. Natural precipitation events have erratic intensity and duration. Under 0.89 mm h^{-1} rain intensity, Gish et al. (2004) found that the mass flux breakthrough curve was dominated by matrix flow (i.e., the preferential flow pathways were not hydraulically active). Therefore, many similar field experiments of this type must be conducted at different infiltration rates and durations to determine the exact relationships among these six parameters. This was why we hesitated to use the regression relationships from Fig. 7 to simplify Eq. [4] into an expression with a single parameter.

The shapes of the equivalent pore spectra of the first irrigation event are shown in Fig. 6. The radius of the largest pore to transport 2,6-DFBA was approximately 20 μm, while the smallest for bromide was around 2.8 μm. These spectra confirmed the observation of Kung et al. (2005) that a range of new pores becomes hydraulically active simultaneously as a soil profile becomes wetter. For example, the equivalent radius of the largest pore to transport the third tracer, *o*-TFMBA, was 13.3 μm. According to the conventional conceptualization (Hutson and Wagenet, 1995), only new pores with equivalent radii larger than 13.3 μm would be active as the irrigation continues and the soil profile becomes wetter. However, when the fourth tracer was applied, new pores ranging from 4.5 to 20 μm became simultaneously hydraulically active.

Figure 6 also shows that fewer and fewer large pores are active in transporting those tracers applied at later times. For example, the maximum amplitude of the

Table 3. Parameters of pore spectra for four sequentially applied tracers from the first irrigation event.

Tracer	α	η	γ	r_1	r_2	A
2,6-DFBA	6.35	2.79	12.2	4.28	9.17	9.45E+07
o-TFMBA	5.27	3.91	18.2	3.60	7.15	1.49E+08
PFBA	4.07	5.32	31.1	3.15	5.23	2.12E+08
Bromide	3.13	8.08	53.9	2.95	4.08	2.46E+08

Table 4. Parameters of pore spectra for four tracers from the second irrigation event.

Tracer	α	η	γ	r_1	r_2	A
2,6-DFBA	3.13	8.08	53.9	2.92	3.89	3.15E+07
o-TFMBA	3.13	8.08	53.9	2.95	3.89	3.35E+07
PFBA	3.13	8.08	53.9	2.89	3.88	2.92E+07
Bromide	3.13	8.08	53.9	2.89	3.72	1.97E+07

Table 5. Parameters of pore spectra for four tracers from the third irrigation event.

Tracer	α	η	γ	r_1	r_2	A
2,6-DFBA	3.13	8.08	53.9	2.82	3.79	2.83E+07
o-TFMBA	3.13	8.08	53.9	2.82	3.77	3.26E+07
PFBA	3.13	8.08	53.9	2.79	3.81	2.89E+07
Bromide	3.13	8.08	53.9	2.85	3.66	1.96E+07

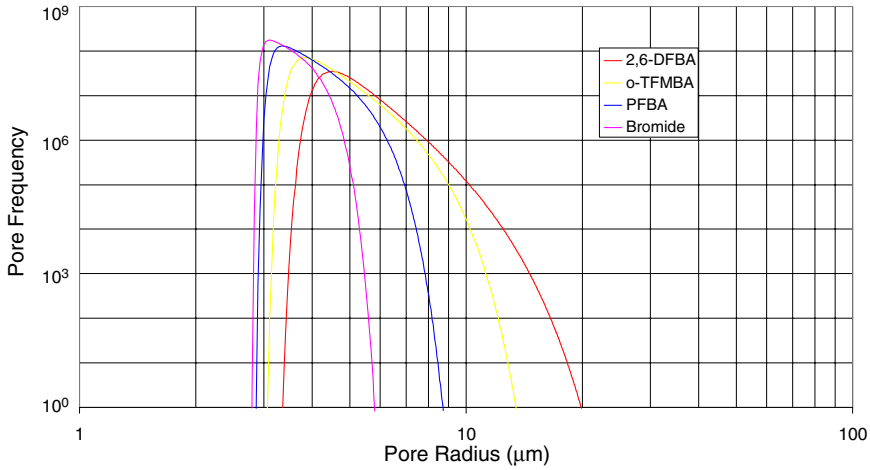

Fig. 6. Pore spectra with parameters (Table 3) based on best fit of four sequentially applied tracers mass flux breakthrough patterns from Kung et al. (2000a).

spectrum of the fourth tracer 2,6-DFBA (3.9×10^7) was more than four times lower than that of the first tracer bromide (1.7×10^8). Nevertheless, because the volumetric water flux in a capillary pore is proportional to the fourth power of the equivalent pore radius, Fig. 8 shows that the volumetric water flux distributions of the four spectra have similar amplitude at the peaks. Convective chemical mass flux through capillary tubes was proportional to the volumetric water flux (Kung et al., 2005). Thus, the larger pores played a more important role in

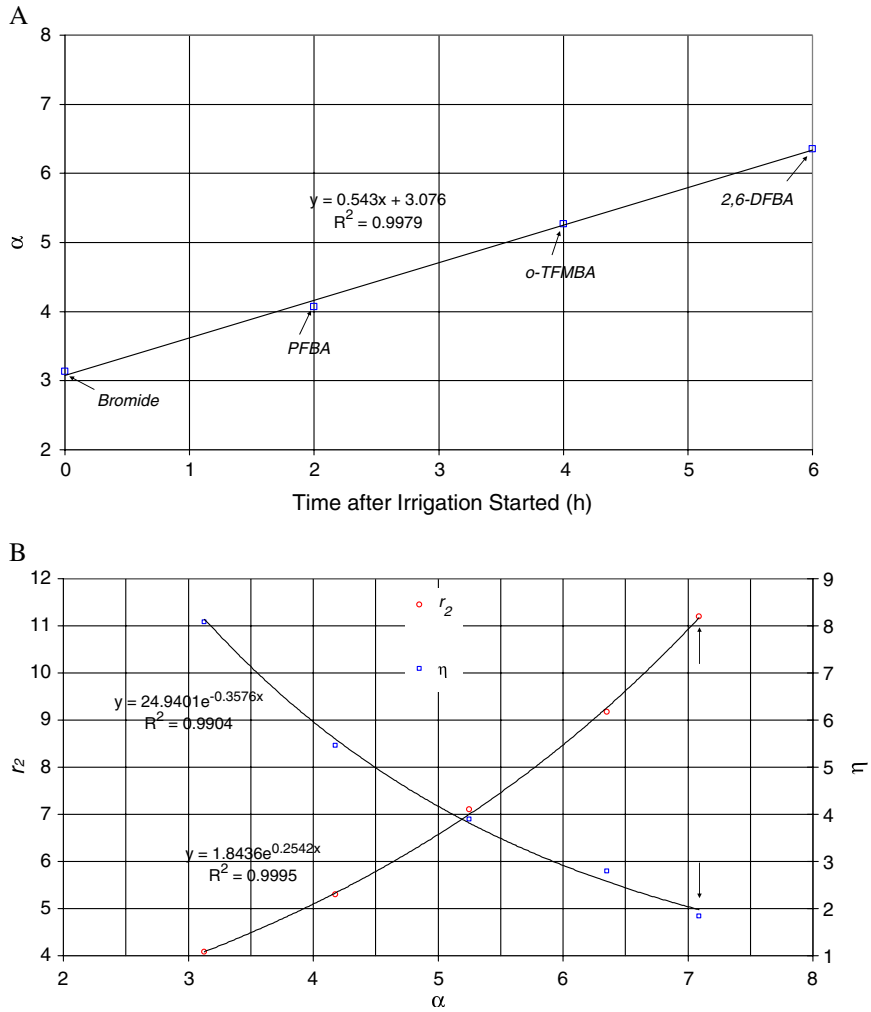

Fig. 7. Continued on next page.

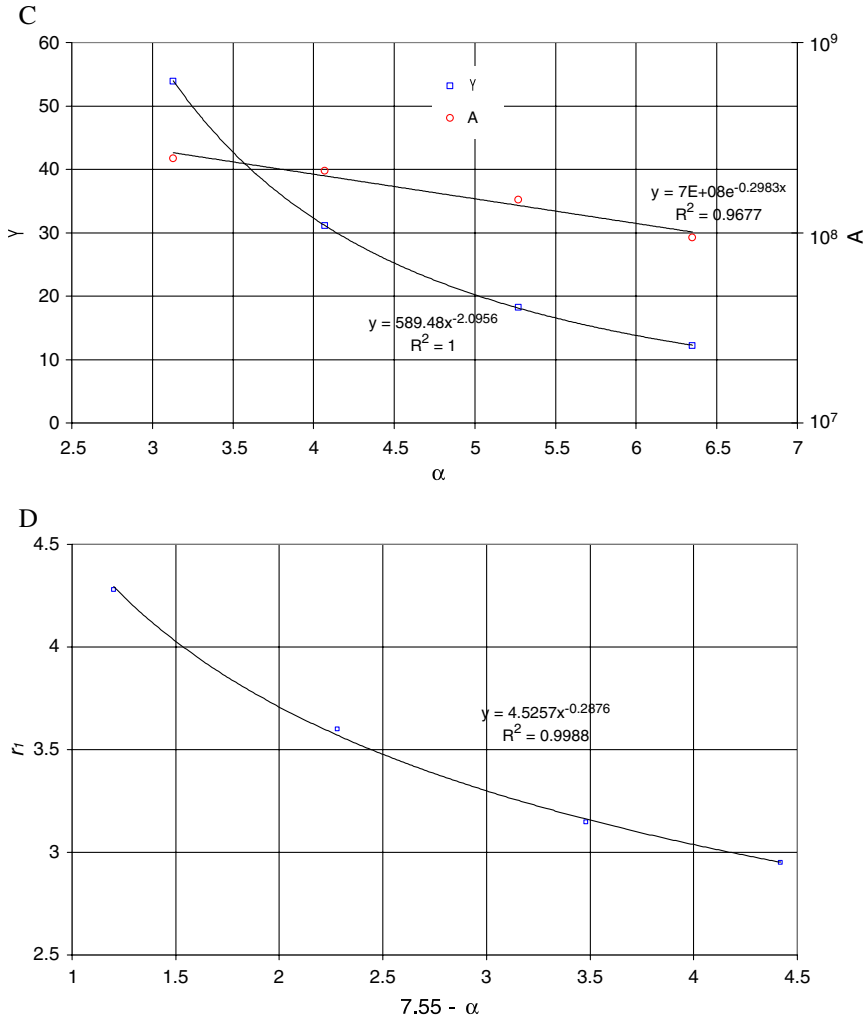

Fig. 7. The regression relationships among the six parameters of pore spectra in Tables 3 through 5. Figure 7A indicates that α is linearly related to the time when a tracer was applied. Figures 7B, 7C, and 7D show that the other five parameters are related to α. Arrows within Fig. 7B represent data acquired at 4.4 mm h^{-1} steady-state infiltration (Kung et al., 2005).

determining the total convective mass flux as a soil profile became wetter. Therefore, about 20% of the total applied 2,6-DFBA was leached out, compared with only 7% of the applied bromide.

From the spectra shown in Fig. 6, it seems that a tracer applied later does not enter some of the smaller pores used to transport an earlier applied tracer. For example, smaller pores with equivalent pore radii ranging from

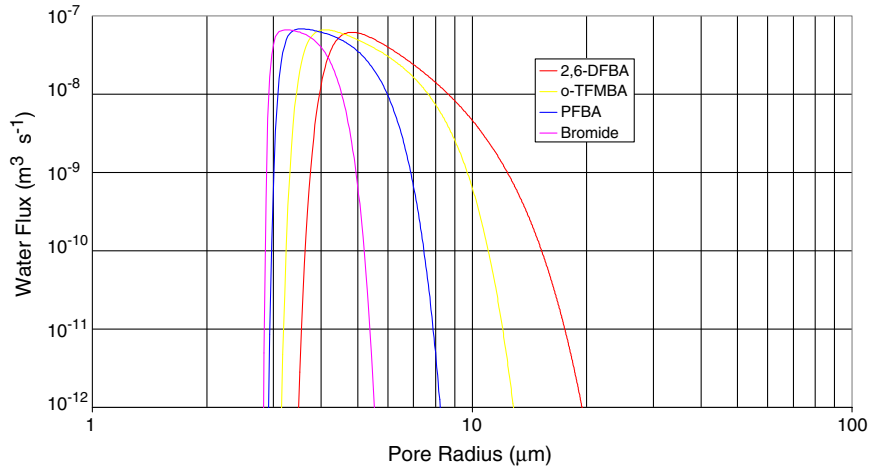

Fig. 8. Volumetric water flux of pores with spectra shown in Fig. 6.

2.8 to 3.4 μm were active in bromide transport, but not for 2,6-DFBA. This is counter-intuitive, because although the fourth tracer 2,6-DFBA was applied at the sixth hour after irrigation started as the soil profile became wetter, the smaller pores active to transport bromide should still be active to transport 2,6-DFBA. There are two potential explanations for this discrepancy. First, the soil surface was dry when the bromide pulse was applied. As a result, there were many small empty pores near the soil surface with negative matric potentials. Because of this matric suction, the rate of initial infiltration into these small pores was high. As irrigation continued, these small pores quickly became saturated, their matric suction greatly diminished, and, hence, their role in the total infiltration was greatly reduced. Hence, the impact of small pores on transport of tracers applied later was greatly reduced. Second, the time available to chemical transport through these small pores was shortened when a tracer was applied later. Because irrigation stopped at the 10th hour, 2,6-DFBA had only 4 h to be transported through the small pores to the water table, while bromide had 10 h. The 2,6-DFBA that entered smaller pores with equivalent pore radii ranging from 2.8 to 3.4 μm simply had not reached the water table when irrigation stopped. The pore frequency in Fig. 6 only reflects those pores that contribute to tracer breakthrough measured in the tile drain. Therefore, small pores with equivalent pore radii ranging from 2.8 to 3.4 μm were not reflected in the 2,6-DFBA spectrum.

The fitted mass flux breakthrough curves in Fig. 1 were nearly identical to the measured mass flux breakthrough curves, except for the tails. Similarly, the tailing was underpredicted in Fig. 2 and 3. Generally speaking, instead of being −3 on log-log scale, the measured tails had slopes gradually changing from −3 to −2. This was because the indirect method proposed by Kung et al. (2005) was developed to quantify equivalent pore spectrum when tracer breakthrough was under steady-state infiltration. In our experimental design, chemical transport was under transient conditions. When irrigation stopped at the 10th hour, a meniscus would immediately form at the top of each pore at soil surface to create a negative matric potential. Because menisci of smaller pores cause more negative matrix potential, some water and tracers in the larger pores would be redistributed laterally into the smaller pores, instead of draining down from their larger pores. This redistribution was beyond the three governing equations (i.e., Eq. [1], [2], and [3]) proposed by Kung et al. (2005).

All bromide applied before the first irrigation event entered into the small pores. The fact that the slope of the entire bromide tail was −3 suggested that as water redistributed laterally from larger pores into the smaller pores after irrigation stopped, this water probably behaved like the infiltration water entering from the top of the small pores. During the second and the third irrigation events, some tracers applied at 2, 4, and 6 h in the first irrigation event had already entered into the smaller matrix pores. As a result, both Fig. 2 and 3 show that the mass flux patterns of these three tracers have tails with slope of −3 initially. If all tracers had entered into soil matrix pores, the entire tails of mass flux patterns for these tracers from the second and the third irrigation events should be similar to that of bromide from the first irrigation event. The fact that the entire tails of the mass flux breakthrough patterns of four tracers did not have slopes of −3 during the second and the third irrigation events suggested the existence of some undetermined mechanism influencing the chemical transport.

The parameters for fitted breakthrough curves for the second and the third irrigation events are shown in Tables 4 and 5. It is intriguing that α, γ, and η of all tracers in Tables 4 and 5 are identical to those of the bromide in Table 3. Note that α, γ, and η dictate the overall shape of a pore spectrum, while r_1 and r_2 determine the location of the pore spectrum and A determines the amplitude of the pore spectrum. The fact that α, γ, and η became constant in the second and the third events suggested that after most of the tracers had entered the small matrix pores, the overall shape of the pore spectrum of macropore-type preferential flow pathways would no longer change. The pore spectra with parameters in Tables 4 and 5 are shown in Fig. 9 and 10. The overall

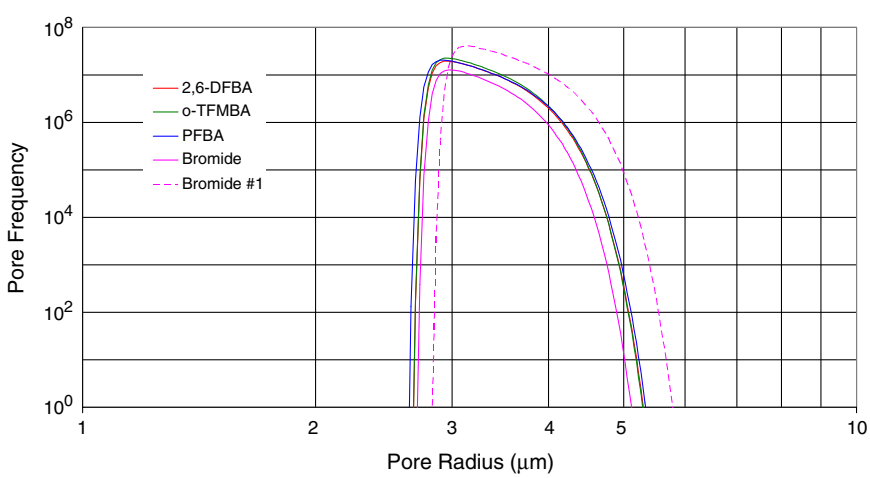

Fig. 9. Pore spectra with parameters (Table 4) based on best fit of four tracers mass flux breakthrough patterns from the second irrigation event. Bromide #1 (broken line) is the pore spectrum of bromide from Fig. 6.

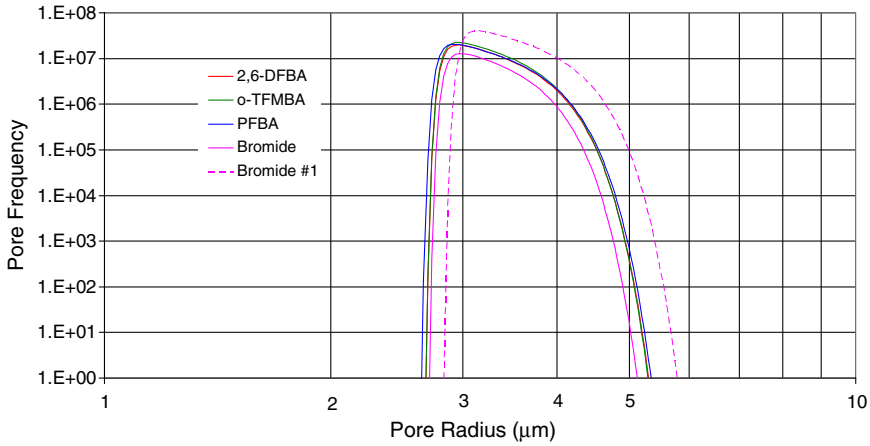

Fig. 10. Pore spectra with parameters (Table 5) based on best fit of four tracers mass flux breakthrough patterns from the third irrigation event. Bromide #1 (broken line) is the pore spectrum of bromide from Fig. 6.

trend indicated that during the subsequent precipitation events, only the position of the pore spectrum gradually shifted toward the left, and the amplitude of the pore spectrum would gradually decrease. The clear trends shown in Tables 4 and 5 again demonstrate that the parameters of fitted pore spectra are not random combinations of numbers but have definable trends.

The fitted initial mass flux breakthrough patterns shown in Fig. 1 are nearly identical to the measured patterns from the first irrigation event. However, the fitted initial mass flux breakthrough patterns of the second (Fig. 2) and the third (Fig. 3) irrigation events are different from the measured patterns during the first 2 h of the breakthrough (i.e., the measured breakthrough patterns had faster chemical arrival to the drain tile). This was likely because there was a background concentration of the tracers (remaining from the previous irrigation event) around the tile drain at the beginning of the second and the third irrigation events. This background concentration during the first 2 h was almost a constant and, since mass flux was calculated by multiplying the measured concentration of the chemical with the tile flow rate, the initial slope of measured tracer mass flux was dictated by the initial slope of the tile flow. Figure 11 shows that, unlike the four sequentially applied tracers, nitrate concentration during the first irrigation event was essentially flat. We did not apply nitrate in this study, and nitrate recovered in tile flow was residual from previous treatments and mineralization. Because tile flow did not increase until about the third hour after the irrigation started, the initial flat concentration reflected nitrate stored in the water table near the tile line. Similarly, the initial flat tracer background concentrations during the first 2 h during the second and the third events were from the water table near the tile line, instead of being leached out from soil surface. Therefore, the mismatch of the initial mass flux breakthrough patterns shown in Fig. 2 and 3 was because the tile sampling protocol would pick up the background tracers from the previous irrigation event.

Most astonishingly, when the parameters α, r_2, and η from a tracer mass flux breakthrough pattern measured by Kung et al. (2005) are plotted on Fig. 7B (their data points are indicated by arrows), their data points align almost perfectly with the trends of our data. It is important to emphasize that the tracer mass flux breakthrough patterns from Kung et al. (2005) were measured under 4.4 mm h^{-1} steady-state condition in southeastern Wisconsin on a site with 3 to 4% organic matter, while those from the present study were measured under transient conditions from southeastern Indiana with approxi-

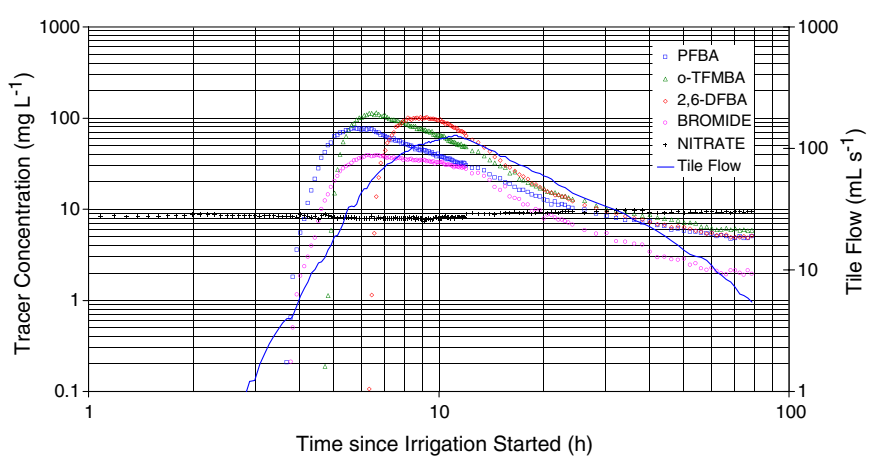

Fig. 11. Tile flow and concentration breakthrough patterns of four tracers and nitrate from Kung et al. (2000a).

mately 1% organic matter. The only similarities were that both sites had silt loam soils and were under no-till corn–soybean rotation.

Parameters α, r_2, and η defined the right (larger) end of the pore spectrum, which determined how the large macropore-type preferential flow pathways became hydraulically active. The larger macropore-type preferential flow pathways likely dictate the leaching potential of reactive chemicals (e.g., pesticides) and pathogens (e.g., bacteria). The fact that the relationships among α, r_2, and η from a 4.4 mm h^{-1} tracer experiment by Kung et al. (2005) aligned with ours strongly suggests a universality in the parameters describing how the large macropore-type preferential flow pathways become hydraulically active. The parameters derived from one site probably could be used to predict transport of chemicals and pathogens through macropore-type preferential flow pathways in another site as long as the soil texture, tillage practices, and crop management of the two sites are similar. This finding is surprising and, yet, may be comprehended with a highway engineering analogy: The large macropore-type preferential flow pathways are generally created by the "soil engineers" such as roots and soil-dwelling macrofauna. To the transport of chemicals and pathogens, these large macropore-type preferential flow pathways are equivalent to a highway system. Because federal highways are built by highway engineers according to identical standards, there is essentially no difference when driving at 65 mph on federal highways through southeastern Wisconsin and southeastern Indiana.

The other parameters A, r_1, and γ from Kung et al. (2005) were not comparable with those derived from our study. This was because A, r_1, and γ were determined by the frequency of the smaller pores. The tracer mass flux breakthrough patterns from Kung et al. (2005) were measured under steady-state infiltration when all pores in the smaller end of the pore spectrum were hydraulically active. As a result, their A, r_1, and γ were representative. Our experiments were conducted under transient conditions and irrigation was terminated at the tenth hour. Although most of the pores in the smaller end of the pore spectrum were hydraulically active, 10 h was not long enough for all tracers to move through these smaller pores to groundwater.

The three equations derived by Kung et al. (2005) describe convective mass flux through individual capillary tubes by gravitational potential gradient under a steady-state infiltration condition without lateral mixing. Although the soil profile was under an unsaturated condition, they envisioned that each hydraulically active preferential pathway was under a saturated condition. In other words, a chemical pulse would only enter saturated pores and be transported by a gravitational potential gradient. Under transient infiltration conditions, water and solute would enter unsaturated pores by both gravitational and matric potential gradients which enhance lateral mixing as a soil profile becomes wetter. The largest pore radius shown in Fig. 6 is approximately 20 μm. The capillary rise in a 20-μm capillary tube is 0.76 m. The maximum depth to perched water table in our experimental site was 0.9 m. Therefore, although our experiments were conducted under transient conditions in unsaturated soil, most of the preferential flow pathways were at least partially filled with water, instead of being completely empty. As a result, the impact of the matric potential gradient on the initial infiltration was probably not significant. In arid regions where macropore-type preferential pathways might be completely empty, the impact of matric potential gradients on chemical mass flux through macropore-type preferential pathways must be considered and another set of governing equations needs to be derived.

SUMMARY

Mass flux breakthrough patterns of four tracers were measured under transient flow conditions and modeled. Our analysis suggested that the indirect methodology proposed by Kung et al. (2005) was valid for quantifying the pore spectrum of macropore-type preferential flow pathways under transient flow conditions. Although Shipitalo et al. (1990) and Edwards et al. (1993) had discussed the effect of soil wetness on the initiation of macropore-type preferential pathways, our analysis demonstrated how pathways with increasingly larger equivalent pore radii became hydraulically active. The distinct relationships among the six parameters describing the pore spectra clearly demonstrated that the indirect methodology proposed by Kung et al. (2005) has predictive value. As a result, it is an attractive alternative to replace the conventional deterministic approach (by solving the Richards equation and the convective–dispersive equation) to predict solute transport through macropore-type preferential flow pathways in areas where these pathways are partially saturated. More field experiments are needed to accurately determine the exact relationships among these six parameters under different precipitation intensities and durations.

The parameters α, r_2, and η independently derived from another mass flux breakthrough pattern with a higher infiltration rate aligned almost perfectly with the relationships from our present results. These three parameters dictate the right end of the pore spectrum, which determines how the large macropore-type preferential flow pathways become hydraulically active. Such large macropore-type preferential flow pathways dictate deep leaching of reactive chemicals and pathogens. This suggests that the pore spectra derived from one site probably could be used to predict transport of pesticides and pathogens through macropore-type preferential flow pathways in another site as long as the soil texture, tillage practices, and crop management of the two sites are similar.

ACKNOWLEDGMENTS

Research was partly supported by USDA-ARS Specific Cooperative Agreement 58-1275-9-094 and USDA-NRICGP 96-35102-3773. The views and conclusions contained in this document are those of the authors and should not be interpreted as representing the official policies, either expressed or implied, of the funding agencies. The authors thank Drs.

Hannes Flühler and Hans-Jörg Vogel who offered helpful suggestions and constructive comments.

REFERENCES

Barenblatt, G.I., I.P. Zheltov, and I.N. Kochina. 1960. Basic concepts in the theory of seepage of homogeneous liquids in fissured rocks. J. Appl. Mech. 24:1286–1303.

Barry, D.A., and G. Sposito. 1989. Analytical solution of a convection-dispersion model with time-dependent transport coefficients. Water Resour. Res. 25:2407–2416.

Bear, J. 1972. Dynamics of fluids in porous media. Elsevier, New York.

Beven, K.J., and P.C. Young. 1988. An aggregated mixing zone model of solute transport through porous media. J. Contam. Hydrol. 3: 129–143.

Bowman, R.S., and J.F. Gibbens. 1992. Difluorobenzoates as nonreactive tracers in soil and groundwater. Ground Water 30:8–14.

Buckingham, E. 1907. Studies on the movement of soil moisture. USDA Bureau of Soils, Bull. 38.

Cassel, D.K., M.Th. van Genuchten, and P.J. Wierenga. 1975. Predicting anion movement in Disturbed and undisturbed soils. Soil Sci. Soc. Am. J. 39:1015–1023.

Darcy, H. 1856. Les fontaines publiques de la Ville de Dijon. Dalmont, Paris.

Durner, W., and H. Flühler. 1996. Multi-domain model for pore-size dependent transport of solutes in soils. Geoderma 70:281–297.

Edwards, W.M., M.J. Shipitalo, L.B. Owens, and W.A. Dick. 1993. Factors affecting preferential flow of water and atrazine through earthworm burrows under no-till corn. J. Environ. Qual. 22:453–457.

Gelhar, L.W. 1987. Stochastic analysis of solute transport in saturated and unsaturated porous media. p. 659–700. *In* J. Bear and M.Y. Corapcioglu (ed.) Advances in transport in porous media. Matinus Nijhoff Publ., Boston, MA.

Gerke, H.H., and M. Th van Genuchten. 1993. A dual-porosity model for simulating the preferential movement of water and solutes in structured media. Water Resour. Res. 29:305–319.

Gish, T.J., and W.A. Jury. 1983. Effect of plant roots and root channels on solute transport. Trans. ASAE 440–444, 451.

Gish, T.J., K.-J.S. Kung, D. Perry, J. Posner, G. Bubenzer, C.S. Helling, E.J. Kladivko, and T.S. Steenhuis. 2004. Impact of preferential flow at varying irrigation rates by quantifying mass fluxes. J. Environ. Qual. 33:1033–1040.

Gwo, J.P., P.M. Jardine, G.W. Wilson, and G.T. Yeh. 1995. A multiple pore region concept to modeling mass transfer in subsurface media. J. Hydrol. 164:217–237.

Hutson, J.L., and R.J. Wagenet. 1995. A multiregion model describing water flow and solute transport in heterogeneous soils. Soil Sci. Soc. Am. J. 59:743–751.

Jardine, P.M., G.V. Wilson, R.J. Luxmoore, and J.F. McCarthy. 1989. Transport of inorganic and natural organic tracers through an isolated pedon in a forest watershed. Soil Sci. Soc. Am. J. 53:317–323.

Jaynes, D.B., S.I. Ahmed, K.-J.S. Kung, and R.S. Kanwar. 2001. Temporal dynamics of preferential flow to a subsurface tile drain. Soil Sci. Soc. Am. J. 65:1368–1376.

Jaynes, D.B., R.C. Rice, and D.J. Hunsaker. 1992. Solute transport during chemigation of a level basin. Trans. ASAE 35:1809–1815.

Jensen, K.H., and J.C. Refsgaard. 1991. Spatial variability of physical parameters and processes in two field soils. Part III: Solute transport at the field scale. Nord. Hydrol. 22:327–340.

Ju, S.-H., K.-J.S. Kung, and C. Helling. 1997. Simulating impact of funnel flow on contaminant sampling in sandy soils. Soil Sci. Soc. Am. J. 61:409–415.

Jury, W.A. 1982. Simulation of solute transport using a transfer function model. Water Resour. Res. 18:363–368.

Jury, W.A., G. Sposito, and R.E. White. 1986. A transfer function model of solute transport through soil. 1. Fundamental concepts. Water Resour. Res. 22:243–247.

Khan, A.U.-H., and W.A. Jury. 1990. A laboratory study of the dispersion scale effect in column outflow experiments. J. Contam. Hydrol. 37:119–131.

Kim, Y.-J., C. Darnault, N. Bailey, J.-Y. Parlange, and T.S. Steenhuis. 2005. Equation for describing solute transport in field soils with preferential flow paths. Soil Sci. Soc. Am. J. 69:291–300.

Kladivko, E.J., J. Grochulska, R.F. Turco, G.E. Van Scoyoc, and J.D. Eigel. 1999. Pesticide and nitrate transport into subsurface tile drains of different spacings. J. Environ. Qual. 28:997–1004.

Kung, K.-J.S., M. Hanke, C.S. Helling, E.J. Kladivko, T.J. Gish, T.S. Steenhuis, and D.B. Jaynes. 2005. Quantifying pore size spectrum of macropore-type preferential pathways. Soil Sci. Soc. Am. J. 69: 1196–1208.

Kung, K.-J.S., E. Kladivko, T. Gish, T.S. Steenhuis, G. Bubenzer, and C.S. Helling. 2000a. Quantifying preferential flow by breakthrough of sequentially applied tracers: Silt loam soil. Soil Sci. Soc. Am. J. 64:1296–1304.

Kung, K.-J.S., T.S. Steenhuis, E.J. Kladivko, T.J. Gish, G. Bubenzer, and C.S. Helling. 2000b. Impact of preferential flow on the transport of adsorbing and non-adsorbing tracers. Soil Sci. Soc. Am. J. 64:1290–1296.

Novakowski, K.S. 1992. An evaluation of boundary conditions for one-dimensional solute transport. 2. Column experiments. Water Resour. Res. 28:2411–2423.

Scotter, D.R., and P.J. Ross. 1994. The upper limit of solute transport dispersion and soil hydraulic properties. Soil Sci. Soc. Am. J. 58: 659–663.

Shipitalo, M.J., W.M. Edwards, W.A. Dick, and L.B. Owens. 1990. Initial storm effects on macropore transport of surface-applied chemicals in no-till soil. Soil Sci. Soc. Am. J. 54:1530–1536.

van Genuchten, M.Th., and J.C. Parker. 1984. Boundary conditions for displacement experiments through short laboratory soil columns. Soil Sci. Soc. Am. J. 48:703–708.

van Genuchten, M.Th., D.H. Tang, and R. Guennelon. 1984. Some exact solutions for solute transport through soils containing large cylindrical macropores. Water Resour. Res. 20:335–346.

van Genuchten, M.Th., and P.J. Wierenga. 1976. Mass transfer studies in sorbing porous media: I. Analytical solution. Soil Sci. Soc. Am. J. 40:473–480.

Wierenga, P.J., R.G. Hills, and D.B. Hudson. 1991. The Las Cruces trench site: Characterization, experimental results, and one-dimensional flow predictions. Water Resour. Res. 27:2695–2705.

Williams, A.G., J.F. Dowd, D. Scholefield, N.M. Holden, and L.K. Deeks. 2003. Preferential flow variability in a well-structured soil. Soil Sci. Soc. Am. J. 67:1272–1281.